PROTEINS: Structure, Function, and Bioinformatics 65:984–998 (2006)

Calcium-Binding and Temperature Induced Transitions in Equine Lysozyme: New Insights From the pCa–Temperature "Phase Diagrams"

Sergei E. Permyakov,[1] Tatyana I. Khokhlova,[1] Aliya A. Nazipova,[1] Andrey P. Zhadan,[1] Ludmila A. Morozova-Roche,[1,2] and Eugene A. Permyakov[1]*

[1]*Institute for Biological Instrumentation of the Russian Academy of Sciences, Pushchino, Moscow region 142290, Russia*
[2]*Department of Medical Biochemistry and Biophysics, Umeå University, Umeå SE-90187, Sweden*

ABSTRACT **The most universal approach to the studies of metal binding properties of single-site metal binding proteins, i.e., construction of a "phase diagram" in coordinates of free metal ion concentration–temperature, has been applied to equine lysozyme (EQL). EQL has one relatively strong calcium binding site and shows two thermal transitions, but only one of them is Ca^{2+}-dependent. It has been found that the Ca^{2+}-dependent behavior of the low temperature thermal transition (*I*) of EQL can be adequately described based upon the simplest four-states scheme of metal- and temperature-induced structural changes in a protein. All thermodynamic parameters of this scheme were determined experimentally and used for construction of the EQL phase diagram in the pCa–temperature space. Comparison of the phase diagram with that for α-lactalbumin (α-LA), a close homologue of lysozyme, allows visualization of the differences in thermodynamic behavior of the two proteins. The thermal stability of apo-EQL (transition I) closely resembles that for apo-α-LA (mid-temperature 25°C), while the thermal stabilities of their Ca^{2+}-bound forms are almost indistinguishable. The native state of EQL has three orders of magnitude lower affinity for Ca^{2+} in comparison with α-LA while its thermally unfolded state (after the I transition) has about one order lower ($K = 15M^{-1}$) affinity for calcium. Circular dichroism studies of the apo-lysozyme state after the first thermal transition show that it shares common features with the molten globule state of α-LA. Proteins 2006; 65:984–998.** © 2006 Wiley-Liss, Inc.

Key words: phase transition; thermodynamics; metal binding; ligand binding; thermal stability

INTRODUCTION

Calcium ions are involved in various fundamental biological processes, including muscle contraction, transmission of nerve impulses, vision, cell division, membrane permeability, exocytosis, bone and tooth formation, and many others (reviewed, for example, in Refs. 1–5). Nature has evolved an elaborate array of proteins that specifically interact with Ca^{2+} (Mg^{2+} and monovalent K^+, Na^+ ions) regulating transmission and reception of the Ca^{2+} signal or playing buffering role. Multiple calcium-binding domains were identified (EF-hand and excalibur, C2, annexin, calreticulin, copine, S100, calsequestrin). The species distribution of calcium-binding proteins, according to the comprehensive database of protein families Pfam,[6] shows that EF-hand, C2, annexin, calreticulin, or copine domains spans all eukaryotic kingdoms, while S100 and calsequestrin families are confined to vertebrates and the EF-hand and its Excalibur analog extend even to thermophilic archaea and eubacteria. The most abundant superfamilies of calcium-binding proteins (EF-hand, C2, and annexin) include thousands members, divided into hundreds subfamilies. Despite the abundance of structural information on calcium-binding proteins, the physical and chemical properties of only some of their representatives have been studied in detail. This situation is partially explained by the fact that the overwhelming majority of calcium-binding proteins contain multiple binding sites, which substantially complicates their physico-chemical characterization. The rare cases of the single site cation binding proteins simplify this process and provide a valuable opportunity to study the regularities of behavior of separate cation binding sites.

Abbreviations: CD, circular dichroism; DSC, differential scanning calorimetry; EDTA, ethylenediaminetetraacetic acid; EGTA, ethylene glycol-bis(β-aminoethyl ether)-*N,N,N′,N′*-tetraacetic acid; EQL, lysozyme, isolated from equine milk; HEPES, *N*-[2-hydroxyethyl]piperazine-*N′*-[2-ethanesulfonic acid]; α-LA, α-lactalbumin, isolated from milk.

Grant sponsor: Russian Academy of Sciences; Grant sponsor: Russian Federal Agency for Science and Innovations; Grant number: 02.442.11.7542; Grant sponsor: Russian Fund for Basic Research; Grant number: 04-04-97322; Grant sponsor: Russian Science Support Foundation; Grant sponsor: CRDF; Grant number: RUB2-010001-PU-05; Grant sponsor: Visby Programme of the Swedish Institute.

*Correspondence to: Eugene A. Permyakov, Institute for Biological Instrumentation of the Russian Academy of Sciences, Pushchino, Moscow region 142290, Russia. E-mail: permyakov@ibp-ran.ru

Received 23 May 2006; Revised 2 July 2006; Accepted 9 July 2006

Published online 4 October 2006 in Wiley InterScience (www.interscience.wiley.com). DOI: 10.1002/prot.21159

To completely characterize calcium binding properties of a single site calcium binding protein one should construct its "phase diagram" in coordinates free metal concentration–temperature.[7] This requires to study metal binding at different temperatures and measurement of thermal unfolding of the protein in the presence of various metal concentrations. The diagram of this kind was previously reported for bovine α-lactalbumin (α-LA),[8] which contains a single high affinity calcium binding site (reviewed in Ref. 9). In the present work a free calcium–temperature phase diagram has been constructed for another calcium binding protein, homologous to α-LA,[10] and similarly possessing a single strong calcium binding site,[11] equine lysozyme (EQL).

EQL belongs to the family of c-type lysozymes. Like hen egg white lysozyme, it consists of two domains divided by a deep cleft. One of the domains contains a β-sheet and some α-helical structure (β-domain), while the other one is rich in α-helical structure (α-domain).[12] The property that distinguishes equine (pigeon, canine, and some others) lysozyme from hen egg white lysozyme is its ability to bind calcium. While hen egg white lysozyme does not specifically bind calcium, EQL binds it tightly.[11,13] Similar to the homologous protein α-LA, the calcium binding site in EQL is formed by side chains of three Asp residues and two main chain carbonyls located in the β-domain.[12,14] According to the work of Lyster,[15] pK values of the carboxylic groups in the calcium binding site are 4.9, 4.3, and 4.1. The calcium binding constant of EQL, determined using Ca^{2+}-sensitive fluorescent dyes Fura-2 and Quin-2, is $2 \times 10^6 M^{-1}$ in 0.1M KCl at pH 7.1 and 20°C.[13] Comparable constant ($3 \times 10^6 M^{-1}$) was obtained at similar conditions (pH 7.5 and 25°C) in the work of Desmet et al.[16] Similar values (1.3–2.9) $\times 10^6 M^{-1}$ were obtained by Lyster[15] and Tsuge et al.[17] At the same time the estimation based upon scanning microcalorimetry measurements[18] gave an unexpectedly low value $6 \times 10^3 M^{-1}$ at pH 4.5 and 25°C, which could be due to the partial protonation of the protein's carboxylic groups.[15]

It was shown[18–21] that, in contrast to hen egg white lysozyme and α-LA, in which the α and β domains unfold as a single cooperative unit, in EQL the two domains unfold in two separate cooperative steps. The calcium binding β-domain unfolds at lower temperatures: for apo-lysozyme this transition occurs in the range from 40 to 44°C, which is significantly higher than the half-transition temperature for apo-α-LA.[22] The binding of Ca^{2+} increases thermal stability of the β-domain, while the stability of the α-domain is insensitive to calcium. It should be noted that most of the experiments on thermal denaturation of EQL were carried out at pH 4.5 to avoid aggregation of the protein at elevated temperatures at neutral pH values.[18,19] However, since pK values of the carboxylic groups in the calcium binding site of EQL are centered around pH 4.5,[15] this pH is not a prudent choice. Moreover, the use of such acidic pH value does not allow using strong metal ions chelators like EDTA/EGTA for efficient removal of calcium ions from the protein. Since EQL possesses high affinity calcium binding site with dissociation constant in submicromolar range,[13,16] it is evident that, despite all possible procedures and precautions intended to avoid calcium contamination of the protein solutions, most of the experiments reported in literature were actually performed on a partially calcium-loaded lysozyme. Thus, characterization of pure apo-state of EQL is of special interest.

In the present work the detailed pH-dependence of intrinsic tryptophan fluorescence of EQL is reported, demonstrating that the well studied state of the protein at pH 4.5 differs from its state at neutral pH. The ability to use strong calcium chelators at neutral pH for efficient removal of calcium from the protein enabled us to study the pure apo-state of EQL. The phase diagram for EQL in coordinates free calcium concentration–temperature was constructed from the experimental data, which allowed us to get key characteristics of both native and denatured states of the lysozyme, some of which are inaccessible from direct experimental measurements. Comparison of the phase diagrams for EQL and bovine α-LA easily reveals similarities and differences in physico-chemical properties of the proteins. It was found that the thermodynamic behavior of EQL shares many more common features with that of its closest homolog, than was assumed earlier.

METHODS

Materials

Equine lysozyme (EQL) was isolated and purified from equine milk as described earlier.[23] Bovine α-lactalbumin (α-LA) was purchased from Sigma Chemical Co. (St. Louis, MO) and used without further purification. The protein concentrations were evaluated spectrophotometrically, using an extinction coefficient $E_{1\%,\ 280\ nm}$ of 23.5 for lysozyme[16] and $E_{1\%,\ 280\ nm} = 20.1$ for α-LA[24] (18.4 there). All buffers were ultra-grade (Sigma Chemical Co). Calcium chloride standard solution was from Fluka and EDTA standard solution was from Fisher Scientific. All solutions were prepared using nano-pure or distilled, deionized water. Plastics or quartz wares were used instead of glassware to avoid contamination of protein samples with calcium.

Methods

Fluorescence studies were performed on a Cary Eclipse spectrofluorimeter (Varian Inc.), equipped with a Peltier-controlled cell holder. Protein fluorescence was excited at 280 nm. All spectra were corrected for the spectral sensitivity of the instrument and fitted to log-normal curves[25] using nonlinear regression analysis.[26] The positions of the fluorescence spectrum maxima (λ_{max}) were obtained from these fits.

In all fluorescence experiments, the protein illumination time and UV irradiation power level were minimized to avoid UV-induced structural rearrangements.[27,28]

Measurements of pH-dependent changes in protein fluorescence were performed by downward or upward titration of the protein solution from initial pH 6.4 by small aliquots of acid or alkali, respectively, followed by mating of the two branches of pH-dependence. The fluorescence intensity was corrected for concomitant dilution of the solution.

Spectrofluorimetric temperature scans were performed stepwise allowing the sample to equilibrate at each temperature. The average heating rate was 0.5°C/min. Temperature was monitored directly inside the cuvette. The fraction of conversion from the native to the thermally denatured state was calculated as described previously.[29,30]

Scanning calorimetry measurements were carried out on a DASM-4M differential scanning microcalorimeter (IBI RAS, Pushchino, Russia) at a 1°C/min heating rate in 20 m*M* H_3BO_3–KOH buffer, pH 8.3. A pressure of 3 bars was maintained in order to prevent degassing of the solutions during heating. Protein concentrations were 1.5–1.8 mg/mL. The heat sorption curves were baseline corrected. Protein specific heat capacity (C_p) was calculated as described by Privalov and Potekhin.[31] The partial molar volume and specific heat capacity of fully unfolded protein were estimated according to Hackel et al.[32] Suppression of high frequency noise of the C_p curve was achieved by adjacent averaging of experimental points within 1°C. The absence of distortions in resulting smoothed curves was checked and confirmed. The temperature dependence of C_p was analyzed using non-linear least squares method according to a simple two-state model, assuming that the difference between heat capacities of the denatured and native protein states (ΔC_p) is independent of temperature (all values were normalized by protein molecular weight MW):

$$C_p = C_{p,D} - \Delta C_p/(1+K) + \left[\frac{\Delta H_{VH} + \Delta C_p(T - T_0)}{T(1+K)}\right]^2 K/R, \quad (1)$$

where

$$K = \exp\left[\frac{\Delta H_{VH} - \Delta C_p T_0}{R}\left(\frac{1}{T_0} - \frac{1}{T}\right) + \frac{\Delta C_p}{R}\ln\frac{T}{T_0}\right] \quad (2)$$
$$R = 8.31/MW\ J(g\,K).$$

Here, T is absolute temperature and $C_{p,D}$ is the specific heat capacity of the denatured protein, linearly extrapolated to the transition region. Fitting parameters: ΔC_p, ΔH_{VH} (van't Hoff's enthalpy of protein denaturation), and T_0 (mid-transition temperature).

Circular dichroism (CD) measurements were carried out with a JASCO J-810 spectropolarimeter (JASCO Inc., Japan), equipped with a Peltier-controlled cell holder, using cuvettes with pathlengths of 10 and 1.00 mm for near- and far-UV regions, respectively. Protein concentrations were 30 and 3 μ*M* for near- and far-UV regions, respectively. The small contribution of buffer (20 m*M* H_3BO_3–KOH) was subtracted from experimental spectra. Band width was 2 nm, averaging time 2 s, and accumulation 2. Quantitative estimations of the secondary structure contents were made using the CDPro software package, which includes the programs SELCON3, CDSSTR, and CONTIN (http://lamar.colostate.edu/~sreeram/CDPro).[33] The experimental data in 190–240 nm range were treated by all the three programs, using SDP48 and SMP56 reference protein sets. The root-mean-square deviation (RMSD) between experimental data and theoretical curves, produced by the programs with SDP48 reference set, was less than with SMP56 set, and so only the results obtained with the SDP48 reference proteins were accepted. At the same time, the RMSD between experimental and calculated points upon the use of the SELCON3 program was markedly high, and so the results obtained with the SELCON3 were omitted. Thus, the final secondary structure fractions reported represent the averaged values produced by CDSSTR and CONTIN programs upon the use of the SDP48 reference set.

Temperature scans were performed at several wavelengths simultaneously in a stepwise manner, allowing the sample to equilibrate at each temperature. The average heating rate was 0.5°C/min. Temperature was monitored directly inside the cuvette. Averaging time was 8 s.

Purification of protein samples from calcium ions was done using the Sephadex G-25 gel-filtration method described by Blum et al.[34]

The calcium affinity of protein was measured by means of spectrofluorimetric titration of the Ca^{2+}-free protein with a $CaCl_2$ standard followed by spectrofluorimetric titration of the calcium-loaded protein with a strong calcium chelator (EDTA standard) at a fixed pH. Calculations of the calcium association constant from the experimental data were based on a scheme of competition between a protein (P) and a chelator (Chel) for calcium ions[30,35]:

$$P + Ca^{2+} \overset{K_1}{\leftrightarrow} P \cdot Ca^{2+}$$
$$Chel + Ca^{2+} \overset{K_2}{\leftrightarrow} Chel \cdot Ca^{2+},$$

where K_1 and K_2 are the protein and chelator equilibrium calcium association constants, respectively. The value of K_1 was estimated using nonlinear regression analysis[26] based upon K_2 value calculated according to Schwarzenbach and Flaschka.[36]

RESULTS AND DISCUSSION

pH Dependence of Lysozyme Intrinsic Fluorescence

Although calcium-binding lysozymes have been studied for decades, information about their pH-dependent behavior is still very limited. To choose pH conditions most suitable for studies of lysozyme metal binding and stability, we have measured the pH dependence of tryp-

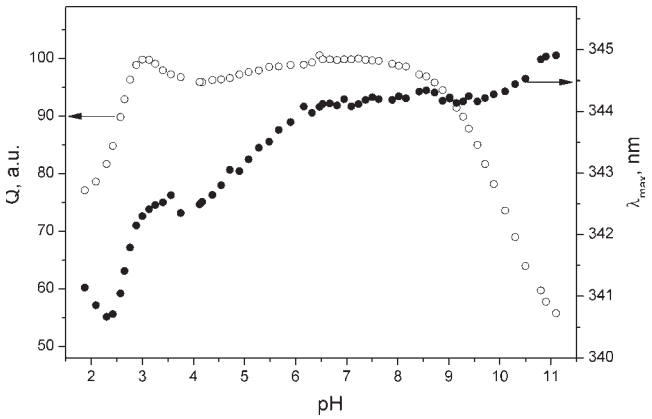

Fig. 1. pH dependence of fluorescence parameters of calcium-loaded lysozyme at 20°C. Lysozyme concentration was 10 μM, $CaCl_2$ concentration was 1 m*M*. Buffer conditions: 3 m*M* glycine, 3 m*M* acetate, 3 m*M* MES, 3 m*M* HEPES, 3 m*M* H_3BO_3. The excitation wavelength was 280 nm. Open circles represent area under fluorescence spectrum (arbitrary units), which is proportional to fluorescence quantum yield, *Q*. Filled circles correspond to the fluorescence spectrum maximum position, λ_{max}.

tophan fluorescence for calcium-loaded (1 m*M* $CaCl_2$) EQL at 20°C (see Fig. 1).

One of the most useful parameters of protein fluorescence spectrum, its maximum position (λ_{max}), reflects polarity and mobility of the polar environment of emitting tryptophans in proteins and often reflects the degree of accessibility of the chromophores to solvent molecules (reviewed by Permyakov[30]). As it is clearly seen from Figure 1, λ_{max} remains constant within the pH region from about 6.4 to 9.7; this implies that the accessibility of the lysozyme tryptophan side chains to water molecules remains essentially invariant in this pH range. At the same time, fluorescence quantum yield (area under fluorescence spectrum) demonstrates slight changes at pH values above 7.6, which indicates that changes in fluorescence quenching properties of tryptophans environment occur in this range of pH. Thus, the pH region from 6.4 to 7.6, characterized by the absence of evident pH-dependent fluorescence changes, seems to be the right choice for physico-chemical characterization of lysozyme. Nevertheless, taking into account that accessibility of Trp residues of lysozyme to water remains invariant at substantially higher pH values, in some of our experiments, pH values up to 8.3 were used. The use of higher pH values allows more complete calcium depletion upon the use of calcium chelators, EDTA/EGTA, which exhibit higher affinity for Ca^{2+} ions at increased pH values. This is of special importance for scanning calorimetry measurements, where rather high (1–2 mg/mL) protein concentrations are used.

The decrease in pH from 6.4 to 3.0 results in a 1.7 nm blue shift of tryptophan fluorescence spectrum (reflecting a decrease in mobility/polarity of environment of some tryptophan side chains) and small (4%) non-monotonic changes in fluorescence quantum yield. There are at least two steps in these spectral changes with apparent pK_a values about 5.2 and 3.4, which seem to be due to protonation of Asp (or Glu) carboxylic groups. According to the work of Lyster,[15] protonation of the carboxylic groups in the calcium binding site of EQL occurs in this pH range (p*K* values 4.9, 4.3, and 4.1). Local plateau observed in pH region from about 3.8 to 4.4 can also be used for structural characterization of lysozyme. pH value 4.5, traditionally used for structural studies of calcium-binding lysozymes, is very close to this range. Nevertheless, pH 4.5 does not allow using of strong calcium chelators, which have very low calcium affinity at acidic pH. Besides, the proximity of pH 4.5 to p*K* values of carboxylates involved in calcium ion coordination[15] makes it quite meaningless for characterization of metal-binding properties of the lysozyme. For this reason the use of neutral pH values is more preferable. While neutral pH promote some aggregation of lysozyme at elevated temperatures,[18,19] it does not prevent studies of the low-temperature thermal transition of lysozyme.

Further acidification of the protein solution from pH 3.0 to pH 2.0 causes a 1.7 nm blue shift of fluorescence spectrum and a marked (22%) decrease in fluorescence quantum yield. The changes seem to reflect a conversion of the protein into the well studied A-state triggered by protonation of carboxylic groups of some other Glu/Asp residues.[37,38] The increase in pH from 7.6 to 11 results in a pronounced (44%) decrease in fluorescence quantum yield and a small (0.7 nm) red shift of the fluorescence spectrum, the later reflecting a denaturation unfolding of the protein.

Thermal Denaturation of Apo-Lysozyme

Previous studies of calcium-binding lysozymes were performed mostly at acidic pH, which prevents the use of strong calcium chelators for efficient removal of calcium traces from protein solutions. As a consequence, most of the thermal denaturation studies of apo-lysozyme reported so far was conducted on a partially Ca^{2+}-loaded protein. To remove the residual calcium, an excess of EDTA was added to the protein at pH ~8. Since Ca^{2+}-binding constant of EQL ($2 \times 10^6 M^{-1}$[13]) is about 2 orders of magnitude lower than that for EDTA at pH 8, an efficient removal of calcium ions is achieved. Scanning microcalorimetry data obtained for EQL in the presence of 1 m*M* EDTA (pH 8.3) are shown on Figure 2(a) (red curve) in comparison with the curve for the protein without addition of EDTA or extra calcium ions (green curve). Although the high temperature heat sorption peak (II) is essentially insensitive to the removal of calcium ions, the low temperature peak (I) demonstrates remarkable changes: it shifts to lower temperatures by about 26°C, and this heat sorption curve closely resembles that for apo-α-LA in analogous conditions.[22] The results of fitting of the low temperature thermal transition of apo-lysozyme to a simple two-state model (Eqs. 1 and 2) are presented in Table I, in comparison with similar data for bovine α-LA.[22] Thermal denaturation of apo-lysozyme, monitored by CD at 291 nm (see Fig. 3), gave

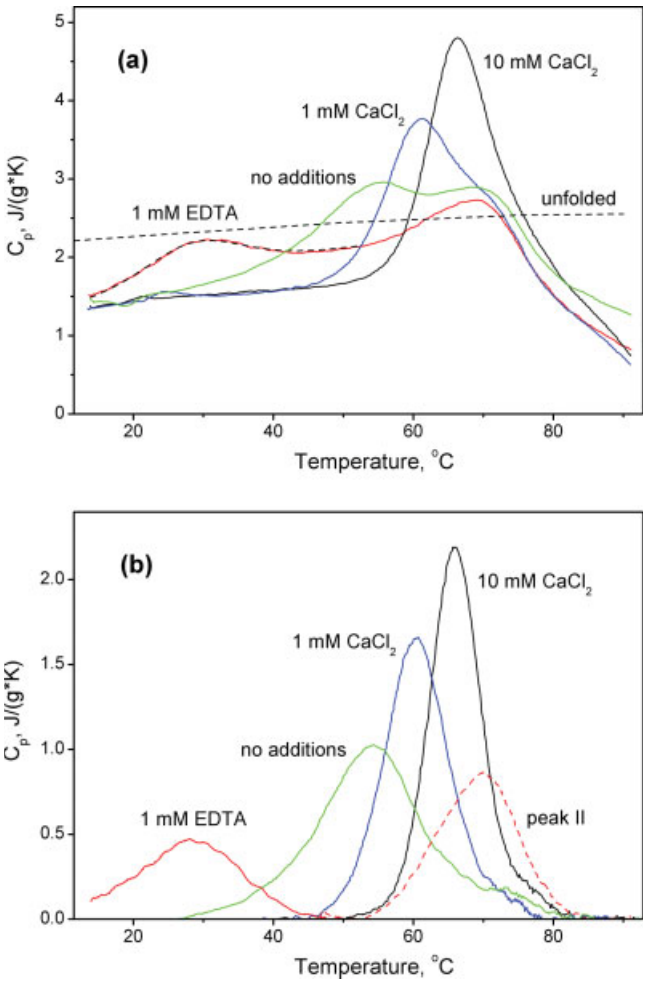

Fig. 2. Specific heat capacity of EQL at various calcium concentrations, estimated from scanning microcalorimetry data (pH 8.3, 20 m*M* H_3BO_3-KOH; heating rate 1 K/min) (a), and deconvolution of the excess heat sorption of lysozyme (b). Concentration of lysozyme was 1.5–1.8 mg/mL. Concentration of calcium ions was controlled by addition of either 1 m*M* EDTA (red), 1 m*M* $CaCl_2$ (blue) or 10 m*M* $CaCl_2$ (black). Green curve depicts reference melting curve of lysozyme without additions. Dotted black curve corresponds to the heat capacity of fully unfolded lysozyme, as estimated according to Ref 32. The melting curve for the apo-protein was fitted to a simple two-state model [dotted curve; see Eqs. (1) and (2)]. The respective excess heat sorption for the low-temperature thermal transition of apo-lysozyme is shown in Figure (b). Deconvolution of the excess heat sorption for other experiments was performed as described in the text.

identical mid-temperature value (24.4°C). About 3°C higher mid-temperature (28.5°C) was observed in intrinsic fluorescence measurements (see Fig. 3). The value may be distorted due to an additional process, revealed by the fluorescence changes at temperatures below 15°C. The fluorescence spectrum maximum position demonstrates here a small (<1 nm) blue shift upon decrease in temperature, which can be attributed to cold denaturation. Analogous effect was reported earlier in differential absorption spectroscopy studies.[20]

Examination of Table I shows that the thermal stability difference between apo-forms of lysozyme and α-LA is about 8°C, which is much less than that reported earlier.[18–20] Consequently, the thermodynamic behavior of lysozyme shares more common features with that of its closest homolog, α-LA, than it was assumed. Certainly, this conclusion cannot be extended to high temperature thermal transition of lysozyme, which is absent in α-LA.

TABLE I. Results of Fitting of the Scanning Microcalorimetry Data for Apo-Lysozyme Presented in Figure 2(a)[a]

Protein	$T_{1/2}$ (°C)	ΔH_{VH} (J/g)	ΔC_p (J/g K)
Apo-lysozyme	25.3	9.3	0.29
Apo-α-LA	17.1	7.9	0.50

[a]According to the simple two-state model [Eqs. (1) and (2)], in comparison with the data for bovine α-LA measured in analogous conditions.[22]

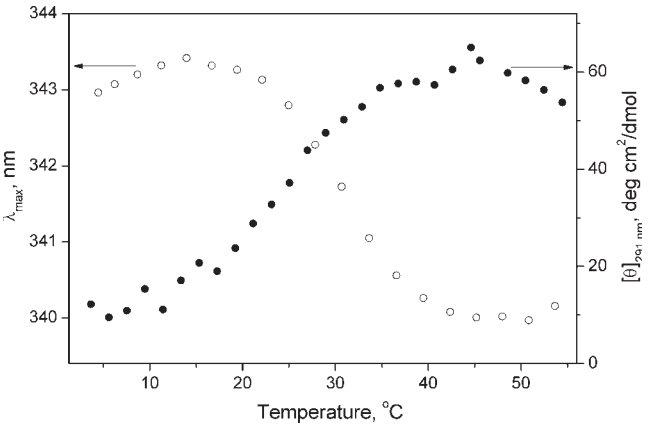

Fig. 3. Low temperature thermal transition of apo-EQL traced by intrinsic protein fluorescence and near-UV circular dichroism techniques. Lysozyme concentration was 7 μ*M* (fluorescence) or 30 μ*M* (CD). Calcium depletion was achieved by addition of 1 m*M* EDTA/EGTA. Buffer conditions: pH 8.0–8.2, 10 m*M* HEPES-KOH (fluorescence) or 20 m*M* H_3BO_3-KOH (CD). Open circles represent the fluorescence spectrum maximum position, λ_{max}. Filled circles correspond to the protein molar ellipticity at 291 nm, $[\theta]_{291\ nm}$.

Comparison of Native and Intermediate States of Apo-Lysozyme

One of the most intriguing features of apo-α-LA is its ability to be converted into classical "molten globule" state upon thermal denaturation of its native state.[39,40] It is of interest whether or not apo-lysozyme demonstrates similar behavior. Strictly speaking, because of its high temperature thermal transition (II) with heat sorption, the intermediate state of lysozyme cannot be considered as a classical molten globule. Indeed, its molten globule-like states possess an extended hydrophobic core based on the native-like interactions of three of its major α-helices in α-domain as it has been found under both equilibrium and kinetic unfolding conditions previously.[37,38,41]

CD technique has proven to be highly efficient both in assessment of protein secondary structure and characterization of asymmetry of environment of aromatic side

chains. The ability of CD to discriminate between destruction of protein tertiary and secondary structures was of high importance in experimental validation of the molten globule state. Figure 4 shows the near- (a) and far-UV (b) CD spectra for native (3°C) and denatured (45°C) apo-lysozyme. Evidently, the thermal transition results in essential spectral changes in both UV regions.

Native apo-lysozyme is characterized by low-intensity structured (extremums at 282, 284.5, 288, 291.5, 295, and 303.5 nm) near-UV spectrum with a positive band from 269 to 300 nm. The absence of a negative band above 275 nm suggests that tyrosine and tryptophan side chains in lysozyme are mostly exposed to the solvent, which is quite unusual, taking into account high hydrophobicity of these residues. This conclusion is corroborated by a very long wavelength position of tryptophan fluorescence maximum (343.0 nm), implying that emitting tryptophan residues in lysozyme are exposed to water molecules. Nevertheless, the observed fine structure of near-UV CD spectrum shows the existence of certain specific contacts of Trp and, possibly, Tyr side chains in lysozyme with neighboring groups. Examination of the crystal structure of apo-lysozyme (2EQL structure of PDB[12]) reveals that only one (W28) of five Trp side chains (28, 63, 64, 108, and 111) is buried, while four others are exposed to solvent. Similarly, all four Tyr side chains (23, 34, 54, and 123) of the protein are highly solvent exposed.

The thermal denaturation makes the near-UV spectrum less structured (only the peak at 287.4 nm persists), significantly enhancing its short wavelength negative band. The spectral changes observed in the region above 294 nm, where a contribution of Tyr residues is excluded, confirm that the symmetry of the environment of Trp side chains changes. The observation is in line with the thermally induced tryptophan fluorescence changes exhibiting 3.5 nm blue shift of spectrum maximum (see Fig. 3). Thus, the environment of emitting Trp residues in the protein becomes less mobile and polar; this is typically related to the lowered accessibility to water molecules. The fact that the intermediate state of lysozyme demonstrates lower accessibility of tryptophan side chains to water than its native state is quite unusual.

High accessibility of aromatic side chains to the solvent is usually a hallmark of protein unfolding. Nevertheless, examination of the far-UV CD spectra of lysozyme [Fig. 4(b)] shows that both native and intermediate states of the protein are characterized by high content of secondary structure. The results of the estimation of the secondary structure contents using the CDPro software package[33] are shown in Table II, in comparison with the analogous data obtained for bovine α-LA, along with the values derived from the crystal structures of the apo-forms.[12,42] All experimental data were satisfactorily described by theoretical curves (data not shown), except for native apo-lysozyme, where apparent deviation in the range from 229 to 234 nm was observed. The discrepancy seems to arise from a Cotton effect of the Trp side chains in the far-UV region and may affect the accuracy of estimation of the secondary structure fractions.

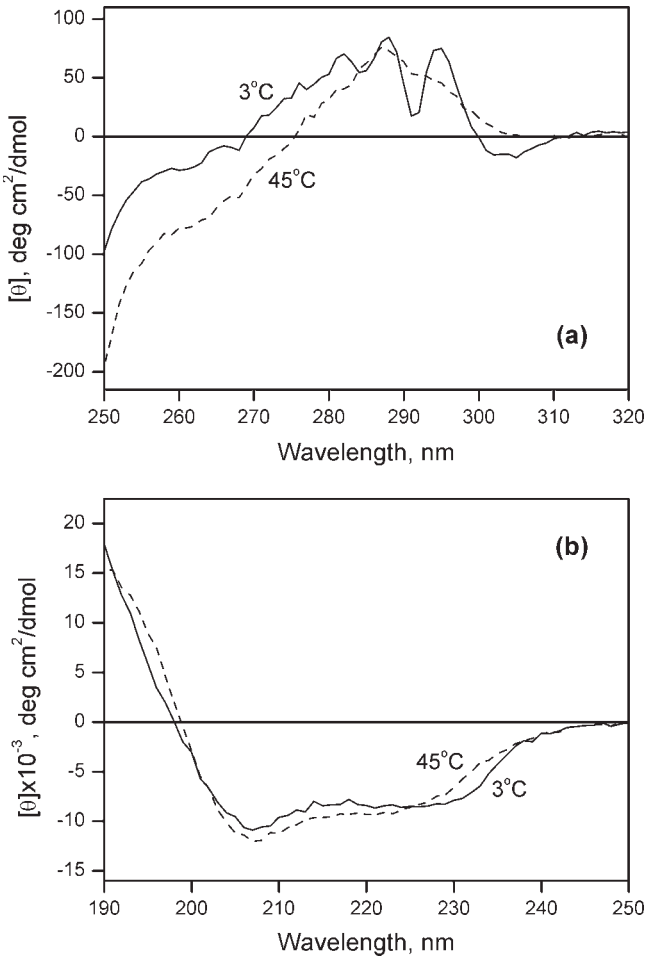

Fig. 4. Near- (a) and far-UV (b) CD spectra for native (3°C) and denatured (45°C) apo-lysozyme. Protein concentrations were 30*M* and 2.8*M* for near- and far-UV regions, respectively. Calcium depletion was achieved by addition of 1 m*M* EGTA. Buffer conditions: pH 8.2, 20 m*M* H_3BO_3-KOH.

As expected, correlation of the CD data for the α-helix contents with the crystal structure (Table II) is much better, than in the case of β-sheets. The discrepancy between structural and CD estimations for α-helices is within 0.5–1.8 residues for 37–38 amino acids involved into α-helical regions, while for β-sheets it amounts to 6.5–9.7 residues per 8–12 amino acids comprising β-sheets. At the same time, CD estimates for total β-sheets content gave identical results for both proteins, while fractions of regular and distorted β-sheet structures differ slightly from each other. Fraction of α-helices, which typically can be predicted by CD much more accurately than β-sheets content, is somewhat less for lysozyme (35 instead of 38.5 residues for α-LA), which is mostly due to the lowered contribution of distorted α-helical regions. Overall, the contribution of unordered structure in native lysozyme is about 19% higher than that in α-LA.

TABLE II. The Results of Estimation of the Secondary Structure Contents (in %) for Native (3°C) and Denatured (45°C) Apo-forms of EQL and Bovine α-LA[a]

Protein	T (°C)	α_R	α_D	$\alpha_R + \alpha_D$	β_R	β_D	$\beta_R + \beta_D$	T	U	α crystal	β crystal
EQL	3	16.65	10.65	27.3	8.5	5.85	14.35	15.85	42.25	28.68	9.3
EQL	45	17.2	13.25	30.45	8.25	6.75	15	17.9	36.45		
α-LA	3	17.25	14.05	31.3	7.95	6.4	14.35	18.8	35.65	30.89	6.5
α-LA	45	16.1	13.5	29.6	9.5	7.05	16.55	17.25	36.5		

[a]Using the CDPro software package,[33] in comparison with the values derived from their X-ray structures.[12,42] CD data for lysozyme used for calculations are shown in Figure 4. Analogous data for α-LA were obtained in identical conditions (not shown). R and D denote regular and distorted α-helix or β-strand. T and U correspond to turns and unordered structures, respectively.

The thermal denaturation of lysozyme causes quite unusual changes in its secondary structure (Table II). It is accompanied with about 12% increase in overall α-helical content (for the most part due to the increase in distorted α-helices content), moderate (5%) enhancement in total β-sheets content (again, due to the distorted structure), and 13% increase of the number of residues involved into turns. Thus, an increase in ordered structure of apo-lysozyme upon thermal denaturation is observed. The unordered structure content decreases by about 16%, which is highly unusual. Such an extraordinary effect could be partially explained by the loss of positive contribution into the far-UV CD signal of some aromatic side chains upon protein denaturation. Nevertheless, the observation of a 3.5 nm blue shift of tryptophan fluorescence spectrum (see Fig. 3), which is indicative of a decrease in exposure of Trp side chain(s) to the solvent, supports the conclusion about formation of extra secondary structure elements upon lysozyme denaturation. In marked contrast, bovine α-LA loses α-helixes (by about 5%) and turns (8%) upon denaturation, while it gains (15%) β-strands. Overall, the contribution of unordered structure increases in this case by about 2%.

Finally, comparison of the thermally denatured (45°C) states of lysozyme and α-LA shows (Table II) that the moderate difference in α-helical contents observed for native proteins substantially decreases (five-fold) upon heating (mostly due to the increase of distorted α-helices content in lysozyme), along with the fivefold decrease of difference in turns content. On the contrary, identical fractions of β-sheets diverge by 10%. Fractions of unordered structure for both proteins become indistinguishable. Thus, the difference in secondary structure contents of denatured forms of lysozyme and α-LA is minimal, as judged by CD, which shows that intermediate state of apo-lysozyme shares structural features of the molten globule state of α-LA. In contrast to the α-LA molten globule, the formation of the lysozyme molten globule from native state seems to be accompanied by formation of extra elements of secondary structure. It should be emphasized that the high-temperature thermal transition of the protein, accompanied with enthalpy change, is not consistent with the classical molten globule model.

Ca^{2+}-Binding Properties of Native EQL

Taking into account that the thermal transition of apo-lysozyme occurs at room temperatures ($T_{1/2}$ ~25°C, see Table I), one should expect that Ca^{2+}-affinity of the protein will change in this temperature interval. To estimate protein calcium affinity, Ca^{2+}-freed lysozyme was titrated with a $CaCl_2$ standard until saturation was reached; it was then titrated with EDTA standard solution. The structural changes accompanying calcium binding and removal from lysozyme were monitored using intrinsic protein fluorescence (see Fig. 5). Calculation of the apparent equilibrium Ca^{2+} association constant K_a from the experimental data was based on a Scheme 1 of competition between the protein and chelator for Ca^{2+} ions. The fluorescent Ca^{2+}-titration experiments performed at different temperatures show (see Fig. 6) that K_a remains substantially constant up to about 30°C, while at higher temperatures it decreases by nearly one order of magnitude per each 10°C up to 50°C. As follows from Figure 2, the thermal transition I of the Ca^{2+}-saturated form begins above 50°C; this implies that the Ca^{2+}-binding experiments at higher temperatures would be affected by a contribution of the thermally denatured Ca^{2+}-loaded state.

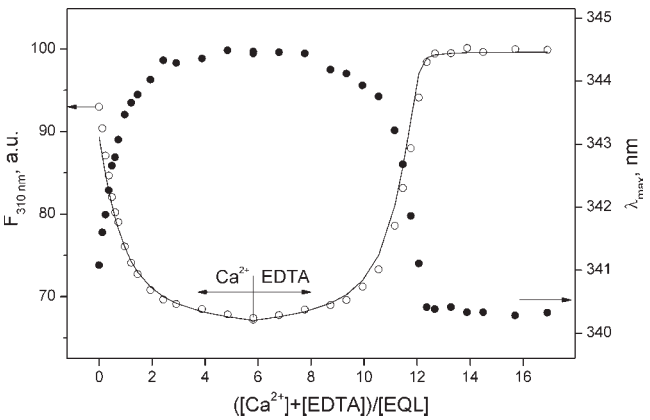

Fig. 5. Spectrofluorimetric titration of purified from calcium EQL by $CaCl_2$ and EDTA at 35°C. The excitation wavelength was 280 nm. The EQL concentration was 8 μM. Buffer conditions: pH 8.03, 10 m*M* HEPES-KOH. Open circles represent the fluorescence intensity at 310 nm in arbitrary units. Filled circles correspond to the fluorescence spectrum maximum position, λ_{max}. The solid curve was fit to the experimental data according to the competitive binding scheme 1 in Materials and Methods.

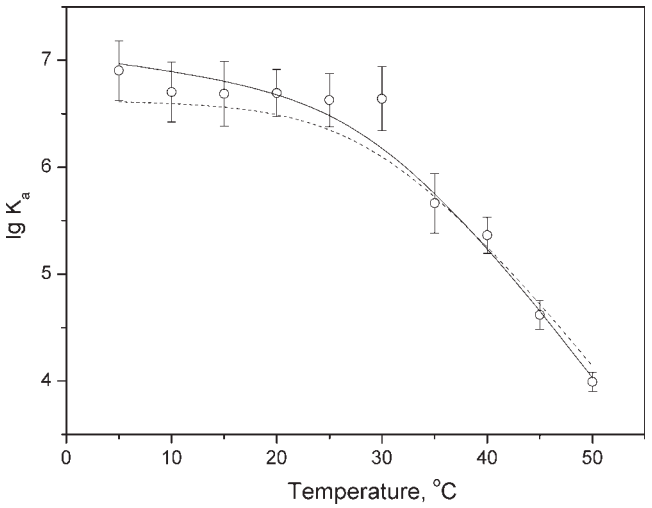

Fig. 6. Temperature dependence of apparent equilibrium calcium binding constant K_a of EQL, determined from spectrofluorimetric titrations by $CaCl_2$ and EDTA (pH 8.03, 10 m*M* HEPES-KOH), as described in Refs. 30 and 35. Protein concentrations were 7–9 μM. The dotted line represents theoretical curve obtained by fitting of the data according to the simplest four-states scheme 2 [see Eq. (8)] in assumption that equilibrium calcium association constant for native protein, K_n, is independent of temperature. The solid line corresponds to the analogous theoretical curve, obtained considering temperature dependence of K_n [Eq. (9)].

The character of the temperature dependence of K_a can be easily described on the basis of the simplest four states scheme (see Refs. 7 and 8):

$$\begin{array}{ccc} & \alpha(T) & \\ N & \leftrightarrow & I \\ + & & + \\ M & & M \\ K_n(T) \updownarrow & & \updownarrow K_u(T) \\ NM & \leftrightarrow & IM \\ & \beta(T) & \end{array}$$

Here, the upper horizontal equilibrium describes thermal denaturation of the apo-protein (conversion of the native "N" state into intermediate "I" state), while the lower horizontal equilibrium corresponds to the denaturation of the metal-bound protein form (conversion of the metal-loaded native "NM" state into metal-loaded intermediate "IM" state). Two vertical equilibria describe the binding of a metal ion "M" to native or intermediate states, respectively. Each of the processes is characterized by its own association constant:

$$\alpha = [I]/[N] \tag{3}$$

$$\beta = [IM]/[NM] \tag{4}$$

$$K_n = [NM]/([N][M]) \tag{5}$$

$$K_u = [IM]/([I][M]) \tag{6}$$

Combining the Eqs. (3)–(6) the following relationship can be easily obtained for the apparent calcium binding constant K_a, measured experimentally:

$$K_a(T) = ([IM] + [NM])/\{([I] + [N])[M]\} = (\beta + 1)K_n/(\alpha + 1) \tag{7}$$

At temperatures below 50°C β is negligibly small and K_a value approaches $K_n/(\alpha + 1)$:

$$K_a(T) = K_n/(\alpha + 1) \tag{8}$$

Knowing $\alpha(T)$ dependence (see Eq. 2 and Table I) the fit of the temperature dependence of K_a (Eq. 8) can be used for a rigorous evaluation of K_n value by using K_n as a fitting parameter. The resulting theoretical curve (corresponding to $K_n = 4.3 \times 10^6 M^{-1}$), shown in Figure 6, satisfactorily describes the experimental data within experimental accuracy. The value of K_n slightly exceeds the earlier estimate of Ca^{2+}-binding constant of EQL ($2 \times 10^6 M^{-1}$) obtained at pH 7.1 and 20°C in 0.1*M* KCl by Nitta.[13] Similar values (1.3–3) $\times 10^6 M^{-1}$ were obtained in Refs. 15–17. The calcium binding constant of EQL evaluated from scanning calorimetry data is about $6 \times 10^3 M^{-1}$ at pH 4.5 and 25°C[18]; this differs from the aforementioned results. Taking into account the p*K* values (4.9, 4.3, and 4.1) of the carboxylic groups in the calcium binding site of EQL,[15] one should expect that the calcium affinity of the lysozyme at pH 4.5 will differ greatly from that observed at neutral pH. Our value of the EQL Ca^{2+} association constant K_n exceeds to a certain extent the literature values, since it represents not an apparent binding constant K_a, which actually coincides with the previously reported constants within experimental accuracy (see Fig. 6), but real thermodynamic constant derived from the multiple Ca^{2+} titration experiments.

Although the theoretical curve describing the $K_a(T)$ dependence, which assumes that K_n is independent of temperature, agrees well with the experimental data, one can notice that the tendency of $K_a(T)$ to decrease with temperature is not totally described. One of the possible reasons of this phenomenon is the temperature dependence of K_n, which can be described based upon the van't Hoff's equation (compare to Eq. 2, assuming that ΔC_p is zero):

$$K_n(T) = K_n(T_0)\ \exp[\Delta H(1/T_0 - 1/T)/R], \tag{9}$$

in which T_0 is an arbitrarily chosen temperature and ΔH is an enthalpy of metal binding. Introduction of an additional fitting parameter (ΔH) results in less discrepancy between the theoretical and experimental curves (see Fig. 6), giving rise to ΔH value of −18 kJ/mol (K_n (300 K) $= 5.6 \times 10^6 M^{-1}$).

Typically experimental studies of enthalpy changes accompanying metal binding by lysozymes and α-LAs are performed in the temperature range where the thermal denaturation of apo-protein is already in progress; this causes very large errors in the experimental estimations of ΔH values due to the fact that the enthalpy of protein renaturation is usually much higher than that for metal binding. For example, Desmet et al.[16] have measured enthalpy change of the binding of Ca^{2+} to EQL at 25°C (pH 7.5) by

microcalorimetry. As follows from Figure 2, at 25°C apo-lysozyme is very close to the middle of thermal transition, while the calcium-bound protein is in the native state. Thus, association of calcium will inevitably cause refolding of the protein, giving a large negative contribution into the measured calcium binding enthalpy. Indeed, the value obtained for ΔH, −76 kJ/mol, seems to be overestimated due to this effect. Analogous examples for α-LA are discussed in Ref. 43.

Even at temperatures close to 0°C the apo-forms of lysozymes and α-LAs are partially denatured due to their low stabilities; this implies that the results of the metal titration experiments will be distorted by an additional enthalpy contribution emerging due to the renaturation of the proteins upon the metal binding. Thus, the direct, microcalorimetric measurements of ΔH will produce values that are only indirectly related to the desired enthalpy values. The method of ΔH estimation, proposed in the present work seems to overcome these objective difficulties.

Since the experimentally accessible accuracy of the calcium titration experiments (see Fig. 6) does not allow determination of ΔH value with high enough accuracy, in all subsequent numerical calculations it will be assumed that K_n is independent of temperature, although the equations mentioned later are valid for any temperature dependence of K_n.

Ca^{2+}-Binding Properties of the Intermediate State of EQL

Since the calcium binding experiments can be successfully explained on the basis of the four-states model [2], we have used this model for further considerations. It turned out that all the experimental data available, except for high-temperature thermal transition of lysozyme, can be appropriately described within the framework of the four-states model.

In the middle of the thermal transition ($T = T_{1/2}$) the following equation takes place[7]:

$$K_u = \{1 - \alpha(T_{1/2}) + K_n[M]\}/\{\alpha(T_{1/2})[M]\} \qquad (10)$$

Hence, knowing the value of mid-transition temperature in the presence of known high concentration of metal ion, one can easily estimate the value of K_u, based upon known $\alpha(T)$ and K_n. In our case the DSC experiment carried out at 10 mM $CaCl_2$ concentration can be used for that purpose [see Fig. 2(a)]. If [M] equals to 0.01M, then the dependence of K_u upon $T_{1/2}$ will look like that shown in Figure 7. Evidently, the half-transition temperature reaches a limit (66.4°C) at vanishingly small K_u. An increase in K_u up to $10M^{-1}$ decreases the mid-transition temperature by just 0.3°C. The proximity of the maximum of the experimentally observed heat sorption peak (66.3°C) to this limit implies that the affinity of the intermediate state of lysozyme for calcium is extremely small, and the accuracy of the estimation of K_u will depend strongly upon the precision of the determination of $T_{1/2}$. Unfortunately, the DSC data are greatly affected

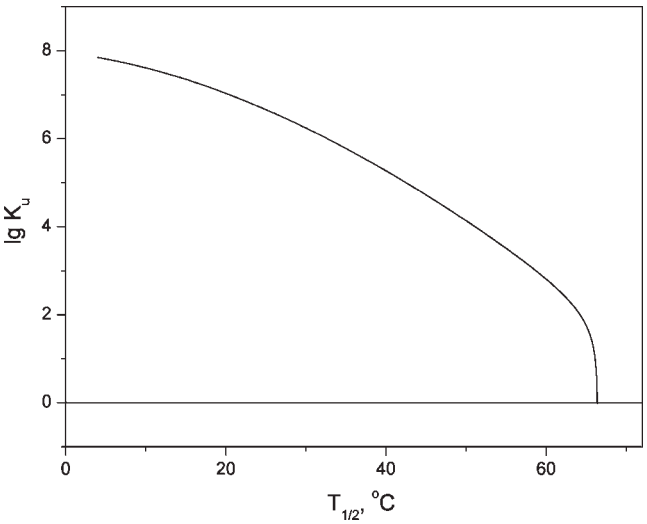

Fig. 7. The dependence of equilibrium calcium binding constant for intermediate state of EQL, K_u (see Scheme 2), on mid-transition temperature $T_{1/2}$ calculated according to Eq. (10) with [M] = 0.01M.

by both aggregation processes and the additional contribution of the high-temperature melting transition II: these effects prevent a precise estimation of $T_{1/2}$. To improve the accuracy of the $T_{1/2}$ determination we attempted to subtract from the total heat sorption curve the excess heat sorption curve of the second thermal transition (virtually independent of calcium content), based upon the DSC curve obtained in the presence of 1 mM EDTA [see Fig. 2(a)]. The respective region of the calorimetric curve for the apo-protein was baseline corrected, using the lowest degree polynomial, producing symmetric residual curve, as a baseline. The resulting excess heat sorption curve of the high-temperature thermal transition [Fig. 2(b), peak II] was subtracted from the calorimetric curve measured in the presence of 10 mM $CaCl_2$. The excess heat sorption for the resulting curve is shown in Figure 2(b) along with the analogous curves produced for two other experiments, conducted at 1 mM $CaCl_2$ or in absence of any additions. The values of mid-transition temperature as a function of calcium content in solution, obtained using this approach, are collected in Table III. Calculation of K_u according to Eq. 10, based upon the value of $T_{1/2}$ = 66.0°C, gives $K_u = 15M^{-1}$. The value is comparable with calcium association constant for free glutamic acid in water, $27M^{-1}$.[44]

The combination of the three found parameters ($\alpha(T)$, K_n, and K_u) is suitable for complete description of the scheme of chemical equilibria (Scheme 2). The remaining fourth parameter of the scheme ($\beta(T)$) can be calculated from the known three parameters based upon the Eqs. (3)–(6).[7]

Validation of the Four-States Scheme 2

So far the Scheme 2 was used for description of thermal denaturation transitions of lysozyme only at extreme calcium concentrations. This helped us to deter-

TABLE III. Comparison of Experimental Values of Mid-Transition Temperatures for Low-Temperature Thermal Transition I of EQL[a]

	$T_{1/2}$	
Ca^{2+} content	Experimental	Theoretical
No additions	54.0	49.2
1 m*M*	60.4	59.2
10 m*M*	66.0	66.0

[a]Estimated from the DSC data presented in Figure 2, with the values derived from consideration of the four-states scheme of chemical equilibria (Scheme 2) [see Eqs. (13) and (14)].

mine with ease all the parameters of the scheme. At the same time, if Scheme 2 is able to describe calcium binding and unfolding equilibria of EQL, then it can be successfully applied to description of thermal transitions occurring at intermediate calcium concentrations as well.

In conditions of known total concentrations of protein (P_0) and metal ion (M_0) the following relationships can be written:

$$[\mathrm{N}] + [\mathrm{NM}] + [\mathrm{I}] + [\mathrm{IM}] = P_0 \quad (11)$$

$$[\mathrm{M}] + [\mathrm{NM}] + [\mathrm{IM}] = M_0 \quad (12)$$

Combining these equations with Eqs. (3), (5), and, (6) the following equation, suitable for determination of [M], can be derived:

$$(K_\mathrm{n} + K_\mathrm{u}\alpha)P_0/\{1 + K_\mathrm{n}[\mathrm{M}] + \alpha(1 + K_\mathrm{u}[\mathrm{M}])\} = M_0/[\mathrm{M}] - 1 \quad (13)$$

Similarly, the apparent degree of conversion from native to the thermally denatured state, observed in experiment, can be expressed via [M]:

$$\Delta_\mathrm{app} = ([\mathrm{I}] + [\mathrm{IM}])/P_0 = \alpha(1 + K_\mathrm{u}[\mathrm{M}])/\{1 + K_\mathrm{n}[\mathrm{M}] + \alpha(1 + K_\mathrm{u}[\mathrm{M}])\} \quad (14)$$

Since, according to fluorescent EDTA-titration experiments (data not shown), the lysozyme sample contained about 0.9–1.0 calcium ions per protein molecule, we were able to estimate the total amount of calcium in the DSC experiments, shown in Figure 2. Consequently, the mid-transition temperatures predicted for these experiments on the base of Scheme 2 can be calculated using Eqs. (13) and (14). Comparison of these values with experimentally observed half-transition temperatures (see Table III) shows that the highest discrepancy (about 5°C) between experiment and the theoretical predictions is observed for measurements in the absence of any additions, where calcium content is estimated with poor accuracy. For 1 m*M* $CaCl_2$ concentration the discrepancy is only about 1°C. Fluorescent melting experiment carried out for lysozyme purified from calcium in the presence of 0.1 m*M* $CaCl_2$, in which uncertainty in contaminating calcium content was much lower than in the DSC measurements, gave mid-transition temperature coinciding with the prediction within 1°C. It should be noted that the previous attempt of description of Ca^{2+}-dependent shift of the thermal transition of EQL based upon the highly straightforward approach not taking into account multiple chemical equilibria occurring in the system resulted in evident underestimation of its calcium affinity.[18] This example is quite representative and clearly demonstrates the necessity to consider all processes taking place in the protein–metal system for its proper description.

Taken together, all available experimental data on calcium binding and thermal stability of EQL are correctly explained using the simplest equilibrium four-states scheme (Scheme 2) The only exception is the high-temperature thermal transition II, which seems to be insensitive to calcium. Its nature require further investigation[37,38,41] and we should not rule out the possibility that further insights of its origin may affect the way the first low-temperature transition of lysozyme is treated. Meanwhile, the behavior of the first transition resembles that for α-LA and can be successfully considered from the same positions. As was shown earlier, α-LA obeys the same scheme of chemical equilibria (Scheme 2).[8]

Phase Diagram for EQL

The use of free metal temperature phase diagrams for studies of single site metal binding proteins was proposed at least 20 years earlier[8] for α-LA, as a highly convenient model system. Presentation of metal-binding protein behavior in free metal concentration, temperature space is one of the most general ways of describing its properties. Despite evident positive properties, it did not meet support from investigators since then. This seems to be related to the necessity to carry out a more detailed physico-chemical study of proteins, including measurements of metal binding at different temperatures and thermal unfolding at different metal concentrations. Moreover, construction of the phase diagrams is coupled to mathematical computing; this further complicates the process. Earlier we presented step-by-step instructions on building the phase diagrams for a set of typical situations encountered in studies of single site proteins,[7] which hopefully will facilitate efforts of investigators interested in this approach. After the developed fashion, the phase diagram of EQL has been constructed based upon the determined parameters of the four-states scheme (Scheme 2).

The complete phase diagram for EQL, shown in Figure 8(a), depicts both regions of predominance of separate protein states and the areas of transitions between them, including lines of half-transitions in (1) calcium and (2) temperature scales.[7] Thus, knowing current temperature and pCa values, the actual protein state can be assessed. Moreover, limits of curves 1 and 2 obviously demonstrate Ca^{2+}-binding affinities of native and denatured states of protein (curve 1, abscissa values) and mid-transition temperatures for apo- and Ca^{2+}-loaded protein (curve 2, ordinate values). Evidently, the area of

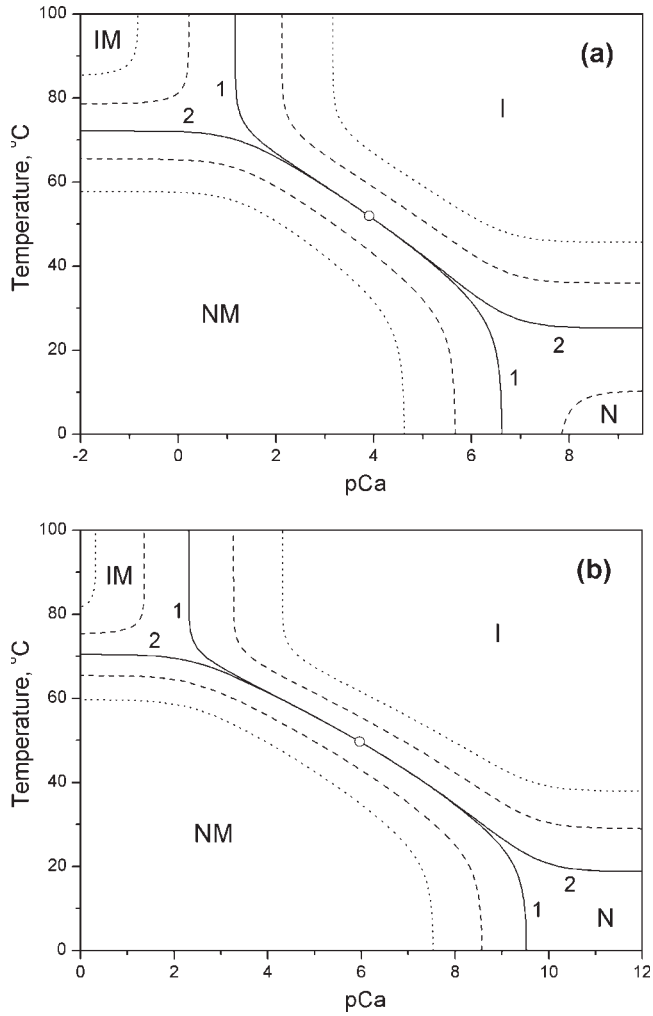

Fig. 8. Phase diagram of EQL (a) and bovine α-LA (b) in the free calcium concentration–temperature space, calculated according to the four-states Scheme 2.[7] Curves 1 and 2 correspond to half-transition for binding of calcium and thermal denaturation (in case of lysozyme, only for lower temperature thermal transition), respectively. The isolines, corresponding to a fixed excess of one protein form over the others, *h*, are calculated using $h = 0.90$ (dashed line) and $h = 0.99$ (dotted line).

the phase diagram with pCa values below 1 should be treated with great cautious, since ionic strength, which was not taken into account in our calculations, may come into play here. Notably, low affinity secondary calcium binding sites were not observed for EQL,[45] suggesting the absence of an additional distortion of the phase diagram at very high calcium concentrations. Neglecting ionic strength effects, one may conclude that lysozyme would be fully Ca^{2+}-saturated at calcium concentrations above 1*M* and would melt at 72°C (compare to 66°C, observed at 10 m*M* $CaCl_2$). The direct experimental evaluation of the K_u or $\beta(T)$ is likely to be hindered upon these high cation concentrations coupled to the ionic strength change related effects or manifestation of some minor low affinity calcium binding sites of the protein. The proposed approach of K_u estimation [see Eq. (10)] based upon experiments fulfilled at low enough calcium concentrations allows overcoming this complication with ease.

Phase Diagram of Bovine α-LA

The use of phase diagrams allows visualization of the differences in physico-chemical behavior of homologous proteins, simplifying their comparison. The phase diagram for the closest homologue of EQL, α-LA, obtained in a similar way, is shown in Figure 8(b). It represents a corrected version of the diagram published earlier,[8] which was based upon just intrinsic fluorescence measurements.

It should be noted that native α-LA possesses essentially higher affinity to calcium ions ($K_n = 4.1 \times 10^9 M^{-1}$), compared to lysozyme and, moreover, to EDTA/EGTA at pH 8. It implies that simple addition of the calcium chelator in 1 m*M* concentration is not enough to remove calcium from the protein in DSC experiments, in which high enough protein concentrations are used, giving rise to low (about 10-fold) molar access of chelator over protein. Since it was found that EDTA/EGTA in millimolar concentration can bind to α-LA,[46] further increase of the chelator concentration should be avoided. Thus, an additional purification of α-LA from calcium is required, as it was done by Veprintsev et al.[22] A more complicated but potentially more powerful approach can be applied. As follows from Eq. (14), the expression for the experimentally observed apparent degree of conversion from native to the thermally denatured state at conditions of very low free metal concentrations ($K_u[M] \ll 1$), which are achieved upon the use of the calcium chelators, may be rewritten as:

$$\Delta_{app} = \alpha/(\alpha + 1 + K_n[M]) \quad (15)$$

This equation can be used for estimation of α:

$$\alpha = (1 + K_n[M])\Delta_{app}/(1 - \Delta_{app}) \quad (16)$$

The change of free metal concentration [M] during the melting experiment can be calculated using the Scheme 1 of competition between the protein and the chelator for metal ions. The protein metal affinity as a function of temperature should be measured experimentally. Thus, knowing Δ_{app}, K_n, and [M], one can determine α. The use of this approach in case of bovine α-LA gave results very similar to those observed experimentally for the protein purified from calcium.[22] The phase diagram, shown on Figure 8(b), is calculated using α estimated from Eq. (16).

As in the case of the EQL phase diagram, the region of the phase diagram of α-LA with pCa values below 1 should be treated with caution since ionic strength effects may emerge here. Moreover, saturation of the secondary low affinity calcium binding site of α-LA upon free calcium concentrations above 1 m*M*[45,47] may cause deviations of the real protein behavior from that predicted by the phase diagram. Neglecting these effects, one may conclude that α-LA would be fully Ca^{2+}-satu-

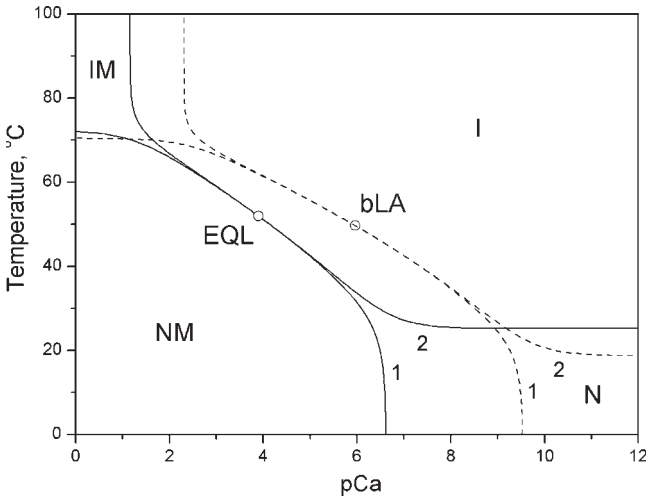

Fig. 9. The comparison of the phase diagrams of EQL (solid curves) and bovine α-lactalbumin (dashed curves), shown on Fig. 8. Only curves 1 and 2 for both proteins are shown.

rated at free calcium concentrations above 0.1*M* and would melt at 70.5°C, which is very close to 72°C predicted for lysozyme.

Comparison of Physico-Chemical Behavior of EQL and α-LA

The key differences in physico-chemical properties of lysozyme and α-LA are easily revealed from consideration of superposition of the curves 1 and 2 of their phase diagrams (see Fig. 9). The numerical values, corresponding to the boundary points of these curves, reflecting principal characteristics of both native and thermally denatured states of the proteins, are collected in Table IV. As was mentioned earlier, the accuracy of K_u determination may suffer due to the very strong dependence of K_u value upon half-transition temperature (see Fig. 7). Importantly, the characteristics of the denatured states are inaccessible in direct experimental measurements due to the necessity to use high calcium concentrations (0.1*M* and higher), which is necessarily coupled to effects related to ionic strength change and manifestation of the secondary low affinity calcium binding site in α-LA.

Interestingly, the differences in the thermal stabilities of the proteins are very small: 6.5°C for the apo-states and about 2°C for the Ca^{2+}-saturated states. Much more prominent differences are observed for their calcium affinities. Native lysozyme possesses 3 orders of magnitude lower affinity for Ca^{2+}, while the calcium affinity for the thermally denatured lysozyme is about 1 order of magnitude lower. Considering that equilibrium calcium association constant is linked to free energy of cation binding ($\Delta G_{Ca} = -RT \ln K$), the observed difference between EQL and α-LA in K_n values can be converted into energetic scale, where it looks less profound: the free energy of calcium binding to EQL amounts to about

TABLE IV. Comparison of the Physico-Chemical Properties of EQL and bovine α-LA[a]

Protein	$T_{1/2,apo}$ (°C)	$T_{1/2,Ca}$ (°C)	K_n (M^{-1})	K_u (M^{-1})
EQL	25.3	72.2	4.3×10^6	1.5×10^1
BLA	18.8	70.5	4.1×10^9	2.1×10^2

[a]Mid-transition temperatures in the Ca^{2+}-free ($T_{1/2,apo}$) and Ca^{2+}-saturated ($T_{1/2,Ca}$) states, equilibrium calcium association constants for native (K_n) and denatured (K_u) protein states (see Scheme 2).

69% from that for α-LA. Calcium ion in primary site of α-LA is coordinated via seven oxygen atoms provided by two water molecules, two carbonyl groups, and three carboxylates.[42,47] Assuming that oxygen atoms involved into calcium coordination equally contribute into free energy of calcium binding[48] and their contribution into ΔG_{Ca} does not differ significantly in EQL and α-LA, one may conclude that the coordination number for Ca^{2+} ion bound to EQL equals to five. Unfortunately, the absence of known crystal structure of calcium-bound state of EQL does not allow checking this conclusion.

The differences in K_n and K_u values are actually related to protein energetics; this allows us to suggest a simple energetic interpretation of the calcium induced changes in stabilities of EQL and α-LA. As follows from the four-states scheme (Scheme 2), the difference ($\delta\Delta G$) between the free energies of denaturation of metal-saturated (ΔG_{Me}) and apo-(ΔG_{apo}) protein forms equals to the difference in the free energies of the metal-binding for denatured and native protein states, which leads to the known equation (see Ref. 7):

$$\delta\Delta G = \Delta G_{Me} - \Delta G_{apo} = RT \ln(K_n/K_u) \qquad (17)$$

According to this equation and Ca^{2+} association constants shown in Table IV, calcium binding to lysozyme is characterized by positive stabilization free energy, which is about 10 kJ/mol lower than that for α-LA. At the same time, the free energy of apo-EQL stabilization (7.1 kJ/mol), as estimated from the known $\alpha(T)$ function, is about twofold higher than the stabilization energy of apo-α-LA (3.3 kJ/mol). The lower stabilization free energy of apo-α-LA becomes apparent from the α-LA phase diagram [Fig. 8(b)], in which the region of 90% predominance of the N state is absent, implying that more than 10% of the protein is denatured in the absence of calcium ions.

Overall, EQL and α-LA represent a quite unique example of proteins possessing very alike thermal stabilities both in apo- and calcium-loaded states, but greatly differing by their affinity to calcium. As follows from Eq. 17, this became possible due to proper K_n/K_u ratio. Thus, proteins possessing highly different K_n values may undergo very similar thermal stability changes upon metal association. Despite evident similarity of certain aspects of physico-chemical behavior of lysozyme and α-LA, one should not forget about the presence of the second high temperature thermal transition in EQL, whose origin remains obscure. Potentially, further

insights into the origins of this thermal transition of lysozyme may affect the way the first low-temperature transition of lysozyme is treated. This intriguing distinctive feature of lysozyme requires further investigation.

In the present work we neglected enthalpies of calcium binding (although the equations used are applicable for any temperature dependencies of the K_n and K_u parameters) and did not consider effect of ionic strength on calcium binding constants and protein stability. This allowed us to simplify the analysis of the system and to emphasize the most significant features of metal- and temperature-induced transitions in lysozyme. More precise measurement of metal binding enthalpies would provide further refinement of the parameters obtained here. However, the direct experimental estimation of these enthalpies is hindered due to the low stabilities of apo-forms of both lysozyme and α-LA, which gives an additional substantial contribution of the protein refolding enthalpy to the total heat effect upon calcium association. The approach proposed here of indirect estimation of the metal binding enthalpy in conditions of very low protein stability [Eqs. (8) and (9)] requires very high accuracy of experimental determination of metal binding constants, which is highly difficult to reach.

EDTA Binding to Lysozyme

In aforementioned experiments the EDTA or EGTA were used as calcium chelators for efficient removal of calcium ions from protein solutions. Strictly speaking, without the use of the calcium chelators, despite application of special procedures, eliminating residual calcium, and all possible precautions, free Ca^{2+} concentration cannot be lowered below $10^{-7}M$, which is not enough to get high-quality apo-state even in the case of lysozyme [see its phase diagram in Fig. 8(a)], which possesses a relatively low affinity for calcium. Thus, the use of calcium chelators is obligatory in studies of calcium binding proteins possessing moderate to high affinity for Ca^{2+} ions. Despite evident convenience of this approach, its reverse side is the possibility of a chelator binding by protein itself; this may affect the protein properties, resulting in controversial results. Thus, chelator binding properties of the protein should be characterized as much as possible.

In our spectrofluorimetric titrations (see Fig. 6), EQL purified from calcium was titrated by $CaCl_2$ standard followed by the titration of the calcium-loaded protein with EDTA standard solution (see Fig. 5). The resulting titration curve was fitted according to the competitive binding Scheme 1. If lysozyme possesses strong EDTA binding site(s), the EDTA-titration part of the titration curve should be elongated relative to the calcium part of the titration curve by the respective number of EDTA molecules bound to the protein. This was not observed in the experiments, implying the absence of EDTA-binding site(s) with association constants exceeding $\sim 10^5 M^{-1}$. To check whether lysozyme possesses low affinity EDTA-binding sites, the spectrofluorimetric

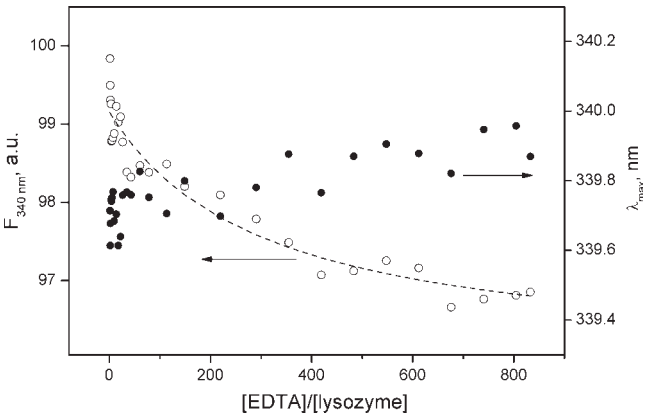

Fig. 10. Spectrofluorimetric titration of EQL by EDTA at 45°C and pH 8.03 (50 m*M* HEPES-KOH). Protein concentration was 12 μ*M*. The excitation wavelength was 280 nm. The dotted line represents theoretical curve obtained by fitting of the fluorescence intensity data according to the simplest single site binding scheme.

EDTA-titration of lysozyme in millimolar range of EDTA concentrations was performed (see Fig. 10). An increase of EDTA concentration up to 10 m*M* was accompanied with a small (~3%) decrease in fluorescence intensity and a tiny (~0.3 nm) red shift of fluorescence spectrum. Fitting of the fluorescence intensity data according to the simplest single site binding scheme gave an apparent EDTA association constant about $3 \times 10^2 M^{-1}$. Lowering of temperature down to 10°C resulted in about threefold decrease of this value. Thus, the use of 1 m*M* concentration of EDTA in previous experiments was accompanied by partial loading of lysozyme with EDTA (EDTA to protein molar ratio from 0.1 to 0.3). Nevertheless, the fact that all experimental data were successfully described based upon the four-states scheme of chemical equilibria (Scheme 2) implies that the weak EDTA binding does not prevent us from obtaining acceptable experimental data. EDTA/EGTA binding with similar association constants was also reported for α-LA.[46]

CONCLUSIONS

In the present work the detailed pH-dependence of intrinsic tryptophan fluorescence of EQL was measured. It was demonstrated that the well studied state of the protein at pH 4.5 differs from its state at neutral pH. The ability to use strong calcium chelators at neutral pH for efficient removal of calcium from the protein enabled us to obtain the pure apo-state of EQL and to study it in detail.

Comparison of the temperature–free calcium phase diagrams constructed for lysozyme and α-LA allowed visualization of the differences in thermodynamic behavior of the two proteins. The thermal stability of apo-EQL (transition I) closely resembles that for apo-α-LA (mid-temperature 25°C) and the thermal stabilities of their Ca^{2+}-bound forms are similar. The native state of EQL has three orders of magnitude lower affinity for Ca^{2+} in

comparison with α-LA while its thermally unfolded state (after the I transition) has about one order lower ($K = 15M^{-1}$) affinity for calcium. CD studies of the apo-lysozyme state after the first thermal transition show that it shares common features with the molten globule state of α-LA. Overall, the data obtained show that EQL is closer to α-LA in its physico-chemical properties, than was assumed earlier.

Overall, the approach to physico-chemical characterization of single site metal binding proteins introduced in Ref. 7, proved to be highly effective in studies of both EQL and α-LA. Because of their low stability in apo-state and presence of an additional thermal transition in case of lysozyme both proteins actually represent fairly complicated systems. The drawbacks of the technique, emphasized in Ref. 7, turned out to affect the quality of the derivable data. The primary interfering factors include (1) the necessity to use strong calcium chelators, which may interact with protein at elevated concentrations, and (2) the strong dependence of the accuracy of the estimation of K_u upon the precision of the determination of mid-transition temperature. Despite certain bottlenecks, the same approach evidently can be successfully used for studies of other single site protein–ligand systems, where ligand represent some low molecular weight substance, which is not transformed upon interaction with the protein. Nevertheless, more universal and robust approaches to the characterization of systems of this kind would further promote popularization of phase diagrams.

ACKNOWLEDGMENTS

We thank W. Noppe for kindly providing us with the sample of equine lysozyme. We are indebted to Dr. S.Y. Venyaminov for helpful suggestions in interpretation of CD spectra and to Prof. R. Kretsinger and Dr. V.N. Uversky for very useful discussion of our work.

REFERENCES

1. Carafoli E. Calcium signaling: a tale for all seasons. Proc Natl Acad Sci USA 2002;99:1115–1122.
2. Haeseleer F, Imanishi Y, Sokal I, Filipek S, Palczewski K. Calcium-binding proteins: intracellular sensors from the calmodulin superfamily. Biochem Biophys Res Commun 2002;290:615–623.
3. Berchtold MW, Brinkmeier H, Muntener M. Calcium ion in skeletal muscle: its crucial role for muscle function, plasticity, and disease. Physiol Rev 2000;80:1215–1265.
4. Clapham DE. Calcium signaling. Cell 1995;80:259–268.
5. Persechini A, Moncrief ND, Kretsinger RH. The EF-hand family of calcium-modulated proteins. Trends Neurosci 1989;12:462–467.
6. Finn RD, Mistry J, Schuster-Bockler B, Griffiths-Jones S, Hollich V, Lassmann T, Moxon S, Marshall M, Khanna A, Durbin R, Eddy SR, Sonnhammer EL, Bateman A. Pfam: clans, web tools and services. Nucleic Acids Res 2006;34:D247–D251.
7. Permyakov SE, Permyakov EA. The use of the free metal—temperature 'phase diagrams' for studies of single site metal binding proteins. Protein J.
8. Permyakov EA, Morozova LA, Burstein EA. Cation binding effects on the pH, thermal and urea denaturation transitions in α-lactalbumin. Biophys Chem 1985;21:21–31.
9. Permyakov EA. α-Lactalbumin. New York: Nova Science Publishers; 2005.
10. Nitta K, Sugai S. The evolution of lysozyme and α-lactalbumin. Eur J Biochem 1989;182:111–118.
11. Nitta K, Tsuge H, Sugai S, Shimazaki K. The calcium-binding property of equine lysozyme. FEBS Lett 1987;223:405–408.
12. Tsuge H, Ago H, Noma M, Nitta K, Sugai S, Miyano M. Crystallographic studies of a calcium binding lysozyme from equine milk at 2.5 A resolution. J Biochem (Tokyo) 1992;111:141–143.
13. Nitta K, Tsuge H, Shimazaki K, Sugai S. Calcium-binding lysozymes. Biol Chem Hoppe Seyler 1988;369:671–675.
14. Mizuguchi M, Nara M, Ke Y, Kawano K, Hiraoki T, Nitta K. Fourier-transform infrared spectroscopic studies on the coordination of the side-chain COO− groups to Ca^{2+} in equine lysozyme. Eur J Biochem 1997;250:72–76.
15. Lyster RL. Effect of calcium on the stability of mares' milk lysozyme. J Dairy Res 1992;59:331–338.
16. Desmet J, Van Dael H, Van Cauwelaert F, Nitta K, Sugai S. Comparison of the binding of Ca^{2+} and Mn^{2+} to bovine α-lactalbumin and equine lysozyme. J Inorg Biochem 1989;37:185–191.
17. Tsuge H, Koseki K, Miyano M, Shimazaki K, Chuman T, Matsumoto T, Noma M, Nitta K, Sugai S. A structural study of calcium-binding equine lysozyme by two-dimensional 1H-NMR. Biochim Biophys Acta 1991;1078:77–84.
18. Griko YV, Freire E, Privalov G, Van Dael H, Privalov PL. The unfolding thermodynamics of c-type lysozymes: a calorimetric study of the heat denaturation of equine lysozyme. J Mol Biol 1995;252:447–459.
19. Morozova L, Haezebrouck P, Van Cauwelaert F. Stability of equine lysozyme. I. Thermal unfolding behaviour. Biophys Chem 1991;41:185–191.
20. Van Dael H, Haezebrouck P, Morozova L, Arico-Muendel C, Dobson CM. Partially folded states of equine lysozyme. Structural characterization and significance for protein folding. Biochemistry 1993;32:11886–11894.
21. Polverino de Laureto P, Frare E, Gottardo R, Van Dael H, Fontana A. Partly folded states of members of the lysozyme/lactalbumin superfamily: a comparative study by circular dichroism spectroscopy and limited proteolysis. Protein Sci 2002;11:2932–2946.
22. Veprintsev DB, Permyakov SE, Permyakov EA, Rogov VV, Cawthern KM, Berliner LJ. Cooperative thermal transitions of bovine and human apo-α-lactalbumins: evidence for a new intermediate state. FEBS Lett 1997;412:625–628.
23. Noppe W, Hanssens I, De Cuyper M. Simple two-step procedure for the preparation of highly active pure equine milk lysozyme. J Chromatogr A 1996;719:327–331.
24. Kronman MJ, Andreotti RE, Vitols R. Biochemistry 1964;3:1152–1160.
25. Burstein EA, Emelyanenko VI. Log-normal description of fluorescence spectra of organic fluorophores. Photochem Photobiol 1996;64:316–320.
26. Marquardt DW. An algorithm for least-squares estimation of nonlinear parameters. J Soc Indust Appl Math 1963;11:431–441.
27. Permyakov EA, Permyakov SE, Deikus GY, Morozova-Roche LA, Grishchenko VM, Kalinichenko LP, Uversky VN. Ultraviolet illumination-induced reduction of α-lactalbumin disulfide bridges. Proteins 2003;51:498–503.
28. Vanhooren A, Devreese B, Vanhee K, Van Beeumen J, Hanssens I. Photoexcitation of tryptophan groups induces reduction of two disulfide bonds in goat α-lactalbumin. Biochemistry 2002;41:11035–11043.
29. Permyakov EA, Burstein EA. Some aspects of studies of thermal transitions in proteins by means of their intrinsic fluorescence. Biophys Chem 1984;19:265–271.
30. Permyakov EA. Luminescent spectroscopy of proteins. Boca Raton: CRC Press; 1993.
31. Privalov PL, Potekhin SA. Scanning microcalorimetry in studying temperature-induced changes in proteins. Methods Enzymol 1986;131:4–51.
32. Hackel M, Hinz HJ, Hedwig GR. A new set of peptide-based group heat capacities for use in protein stability calculations. J Mol Biol 1999;291:197–213.
33. Sreerama N, Venyaminov SY, Woody RW. Estimation of protein secondary structure from circular dichroism spectra: inclusion of denatured proteins with native proteins in the analysis. Anal Biochem 2000;287:243–251.

34. Blum HE, Lehky P, Kohler L, Stein EA, Fischer EH. Comparative properties of vertebrate parvalbumins. J Biol Chem 1977; 252:2834–2838.
35. Permyakov EA, Yarmolenko VV, Kalinichenko LP, Morozova LA, Burstein EA. Calcium binding to α-lactalbumin: structural rearrangement and association constant evaluation by means of intrinsic protein fluorescence changes. Biochem Biophys Res Commun 1981;100:191–197.
36. Schwarzenbach G, Flaschka H. Die komplexometrische titration. Stuttgart: Ferdinand Enke Verlag; 1965.
37. Morozova-Roche LA, Arico-Muendel CC, Haynie DT, Emelyanenko VI, Van Dael H, Dobson CM. Structural characterisation and comparison of the native and A-states of equine lysozyme. J Mol Biol 1997;268:903–921.
38. Morozova LA, Haynie DT, Arico-Muendel C, Van Dael H, Dobson CM. Structural basis of the stability of a lysozyme molten globule. Nat Struct Biol 1995;2:871–875.
39. Dolgikh DA, Gilmanshin RI, Brazhnikov EV, Bychkova VE, Semisotnov GV, Venyaminov SY, Ptitsyn OB. α-Lactalbumin: compact state with fluctuating tertiary structure? FEBS Lett 1981;136:311–315.
40. Kuwajima K. The molten globule state of α-lactalbumin. FASEB J 1996;10:102–109.
41. Morozova-Roche LA, Jones JA, Noppe W, Dobson CM. Independent nucleation and heterogeneous assembly of structure during folding of equine lysozyme. J Mol Biol 1999;289:1055–1073.
42. Chrysina ED, Brew K, Acharya KR. Crystal structures of apo- and holo-bovine α-lactalbumin at 2. 2-A resolution reveal an effect of calcium on inter-lobe interactions. J Biol Chem 2000;275:37021–37029.
43. Griko YV, Remeta DP. Energetics of solvent and ligand-induced conformational changes in α-lactalbumin. Protein Sci 1999;8: 554–561.
44. Martell AE, Smith RM. Critical stability constants. New York: Plenum; 1989.
45. Aramini JM, Drakenberg T, Hiraoki T, Ke Y, Nitta K, Vogel HJ. Calcium-43 NMR studies of calcium-binding lysozymes and α-lactalbumins. Biochemistry 1992;31:6761–6768.
46. Permyakov EA, Murakami K, Berliner LJ. On experimental artifacts in the use of metal ion chelators for the determination of the cation binding constants of α-lactalbumin. A reply. J Biol Chem 1987;262:3196–3198.
47. Chandra N, Brew K, Acharya KR. Structural evidence for the presence of a secondary calcium binding site in human α-lactalbumin. Biochemistry 1998;37:4767–4772.
48. Permyakov SE, Uversky VN, Veprintsev DB, Cherskaya AM, Brooks CL, Permyakov EA, Berliner LJ. Mutating aspartate in the calcium-binding site of α-lactalbumin: effects on the protein stability and cation binding. Protein Eng 2001;14:785–789.